eISSN:3067-6029

JOURNAL OF RESILIENT URBANISM
& SUSTAINABLE DESIGN

2026
Volume 2, Issue 1
Research Article
10.64822/jrusd.v2i1.42

LINKING ENVIRONMENTAL INDICATORS TO HEAT MITIGATION STRATEGIES: A STATISTICAL ANALYSIS OF URBAN HEAT ISLAND AND URBAN DESIGN INDICATORS IN HO CHI MINH CITY

Dieu Thi Minh Nguyen

Institute of Geodesy, Department of Land Management, Technical University of Darmstadt, Germany
Corresponding Author: thi_minh_dieu.nguyen@tu-darmstadt.de

Article History:

- Received 25 November 2025
- Accepted 25 May 2026

Abstract: Urban Heat Island (UHI) poses challenges in rapidly urbanizing cities like Ho Chi Minh City (HCMC). The complexity of urban morphology and the inevitable urban expansion process significantly impact land surface temperature (LST). This study investigates the spatial relationship between LST and seven urban environmental indicators, including both two-dimensional (Normalized Difference Vegetation Index (NDVI), Normalized Difference Built-up Index (NDBI), Normalized Difference Water Index (NDWI), impervious surface, albedo) and three-dimensional metrics (building volume, canopy height). Firstly, using high-resolution remote sensing data, the study models land surface temperature (LST) using Ordinary Least Squares (OLS) and Spatial Error Models (SEM). Secondly, diagnostic tests and k-fold cross-validation are applied to identify the better fit model. Results reveal that the SEM with quadratic NDVI outperforms OLS in addressing spatial autocorrelation and heteroskedasticity. The SEM with robust standard errors is the better fit model for inference and urban design interpretation. NDVI captures the non-linear relationship in HCMC, indicating that a threshold of approximately 0.147 provides a significant reduction in surface temperature. Built-up intensity, imperviousness, and albedo are the dominant warming factors, while an appropriate value of canopy height, water surface, and suitable building volume, combined with green vegetation coverage, can reduce the LST, depending on context. The importance of integrating these indicators as dense, structured green-blue infrastructure is emphasized to enable effective urban cooling in design solutions. The outcome highlights the need for localized urban design interventions to mitigate urban heat.

Keywords: Urban Heat Island, Urban environment indicators, Regression models, Land Surface Temperature, UHI mitigation, Urban design.

1. Introduction

Under the urbanization process, landscape transformation results in higher surface temperatures and atmospheric temperatures in urban areas compared to non-urban surrounding areas, which is known as the Urban Heat Island (UHI) phenomenon (Voogt & Oke, 2003). In the context of climate change, particularly global warming, UHI poses challenges to livable, resilient, and sustainable urban development. As UHI intensifies, energy consumption for cooling rises and reaches peak demand during the hot season. A 1 °C rise in temperature leads to an increase in electrical consumption in both hot climate countries and mild climate countries, by 1.66% and 0.54%, respectively (Tian, 2021). UHI is also associated with worse air quality and heat-related health issues in cities, such as heat stress, increased likelihood of discomfort, or even mortality (Watkins & et al., 2007).

The causes of UHI are diverse, resulting from the complex interaction of urban geometry, urban surfaces, land use, and human activities in different contexts. To address this complexity, urban morphology provides a structured framework of the city system, obtaining a hierarchical view of fundamental physical elements, including streets, street blocks, plots, and buildings. These elements encompass both two-dimensional and three-dimensional characteristics of an urban area, including its material composition (Oliveira, 2016). Urban form significantly shapes the urban microclimate, as defined by Kevin Lynch, through spatial patterns (Yang & Chen, 2020). Key urban design elements, including building density, street canyons, and surface combinations, contribute directly to UHI effects by affecting solar radiation. In particular, the absorption of solar energy and heat exchange on surfaces such as roofs, buildings, streets, and street canyons also modify the UHI dynamic (Hoornweg et al., 2011; Van Hove, Jacobs, et al., 2015; Watkins & et al., 2007). Local urban form and functions are partly influenced by geography and topographical characteristics of an area, which are shown clearly through the airflow and the local circulation system. This local thermal behavior emphasizes the importance of context-specific solutions. Accordingly, analyzing the spatial urban thermal factors and their impacts is crucial to understand UHI for optimizing the urban design guidelines for climate adaptation (Hoornweg et al., 2011; Van Hove, Jacobs, et al., 2015; Watkins & et al., 2007).

It has been demonstrated that vegetation and water surfaces play a crucial role in enhancing the thermal environment of urban areas (He, 2020; Mirzaei, 2015). Green spaces and water bodies serve as buffer zones, helping to moderate urban thermal conditions by reducing surface temperature, roof footprint, and roof facets. Buildings make a significant contribution to heat as they occupy a large proportion of the urban surface and create compact neighborhoods. Roof intervention focuses on materials with high reflectivity and green characteristics. The cool roof system can reduce the solar radiation absorption, particularly the daytime extreme heat. The green roof system can increase evaporation. Another solution is to apply green walls, which can also be considered an upgrade to the air quality of the street. At the street scale, the street canyon is considered to adjust the shadowing and multiple reflections due to the (Height/Width) ratio by lowering building heights and widening streets (Stewart & Mills, 2021b). The urban canyon analysis of a long street with its geometric parameters changes due to aspect ratio, height-to-width ratio, and orientation of streets (Stewart & Mills, 2021c). Hence, identifying indicators related to green and water indices is crucial for enhancing urban design solutions that mitigate heat.

UHI is measured by surface temperature and air temperature. LST is a primary indicator in urban heat investigation as it presents the Earth's surface temperature. Land surface temperature (LST) is derived from thermal radiation. Although they have different measurements and responses to various thermal conditions, LST and air temperature, particularly near-surface temperature, have a strong relationship. Previous research analyzed land use and land cover (LULC) changes in combination with urban metric indicators, including the Normalized Difference Vegetation Index (NDVI), Normalized Difference Built-up Index (NDBI), and Normalized Difference Water Index (NDWI), as well as impervious surface, canopy layer, building materials, and especially albedo. These indicators are representative of both the urban surfaces and urban atmosphere, focusing on built, water, and vegetation coverage (He, 2020), and extracted from remote sensing images, which have been widely used to assess urban thermal patterns through surface characteristics with high spatial resolution and robust imagery (Voogt & Oke, 2003).

Earth Observation satellite sensors have been employed to study UHI since the 1980s. The Landsat Thematic Mapper (TM) and Advanced Spaceborne Thermal Emission and Reflection Radiometer (ASTER) enable detailed analysis of the relationship between the urban environment and surface heat. The vegetation index (NDVI), built area index (NDBI), and water index (NDWI) are ecological indicators considered in the planning process, which contribute to changes in the city landscape and show a significant relationship to LST (Zhang, 2017).

Different models are employed to develop appropriate urban-scale policies for UHI mitigation. While the city-scale model is still limited in providing detailed urban patterns, the micro-scale model is limited in terms of domain size. This requires research to have an appropriate model and methods for better spatial analysis and understanding in specific cases (Mirzaei, 2015). To analyze the relationship between LST and urban environmental indicators, the multilinear regression method has been employed (He, 2020). Traditional linear regression models often yield biased and inconsistent results because they cannot capture spatial dependence and spatial heterogeneity (e. a. Ismaila, 2022a). To capture spatial correlation and spatial heterogeneity, in some case studies, the Spatial Error Model (SEM) has been applied and demonstrated improved performance in comparison to the Ordinary Least Squares (OLS) model (Chen & Zhou, 2004; e. a. Ismaila, 2022b; e. a. Yang, 2022).

As in other high-density urban areas, UHI is a considerable environmental issue in Ho Chi Minh City (HCMC). The rapid rate of urbanization is reflected in the growth of population and spontaneous spatial development rather than urban planning. This process continues to play an important role in urban structure transformation (Son, 2017). Recent research on UHI in HCMC focuses on assessing the urbanization process, land use and land cover, urban planning process, and several indicators, including NDVI, NDWI, NDBI, and impervious surfaces (Cuong & Lin, 2025; Ha & Nguyen, 2023; Le, 2020; e. a. Nguyen, 2023). These studies rely on simple linear regression, focusing on central districts, and are limited in terms of urban three-dimensional data. Using indices such as NDVI, NDWI, and NDBI has shown limitations, so it is recommended to combine other specialized indices for more effective analysis (Tuan & Tran, 2025). Choosing the driving factors that vary across space and time and have significant changes on LST is therefore important. This study aims to investigate the relationship between LST and seven selected urban environmental indicators in both central areas and suburban areas in HCMC. By incorporating two-dimensional indicators, including NDVI, NDBI, NDWI, albedo, and impervious surface, with three-dimensional urban factors, including building volume and canopy height, this study provides a comprehensive representation of surface characteristics and thermal radiation patterns. The variance inflation factor (VIF) was calculated to detect potential multicollinearity among independent variables. The Ordinary Least Squares (OLS) and Spatial Error Model (SEM) were then applied to identify significant driving factors in the spatial variability of heat. Robust standard errors were used to enhance model performance. The study reveals the non-linear relationship between LST and urban environmental indicators, especially NDVI, which was captured more effectively using quadratic analysis. With the selected dataset, it was demonstrated that the SEM with robust standard errors explained thermal influences of urban indicators better than traditional OLS regression due to heteroskedasticity in the urban heat context of HCMC. The influences of indicators enhance understanding of urban spatial thermal dynamics and are translated into urban design solutions for heat mitigation and adaptation strategies in central and peripheral urban zones.

2. Data collection

2.1. Study area

The study area is located in Ho Chi Minh City, Vietnam (Figure 1). Since the late 1980s, Ho Chi Minh City has been a special case in Vietnam experiencing economic reforms, which have significantly influenced socio-economic development. Rapid urbanization has contributed to unsustainable development, particularly due to increasing resource demand associated with population growth (Drakakis-Smith & Dixon, 1997). After 1975, and especially during the period from the 1990s to the early 2000s, service and industrial development generated multiple urban challenges in Ho Chi Minh City, including increased housing demand, environmental pressures such as air pollution, rising energy consumption, and waste management issues (Tan, 2020). These challenges have placed urban sustainability, environmental quality, and livable city development at the center of urban planning discourse.

Historically, inner districts of Ho Chi Minh City developed as high-density urban cores during the colonial period. However, the city structure was also characterized by extensive low-lying tidal systems, canals, and green spaces distributed mainly in the southern, eastern, and northern areas, which limited adaptation to climate-related risks. From the 2000s onward, particularly between 2005 and 2010, the city experienced rapid spatial expansion, with the highest population growth concentrated in peri-urban areas (Downes, 2016).

The study area is divided into five spatial zones (Figure 2) based on urban development orientation and administrative structure. Zone 1 represents the urban core, Zone 2 corresponds to newly developed urban areas, and Zones 3 to 5 represent suburban and peri-urban areas. Specifically, Zone 1 includes central districts such as Districts 1, 3, 4, 5, 6, 8, 10, 11, 12, Tan Binh, Binh Tan, Tan Phu, Binh Thanh, and Phu Nhuan. Zone 2 corresponds to the eastern area including Thu Duc City (Districts 2, 9, and Thu Duc). Zone 3 covers the northern area including Cu Chi and Hoc Mon districts. Zone 4 includes the western area (Binh Chanh), and Zone 5 includes the southern area (District 7, Nha Be, and Can Gio). The study area includes urban built-up land, green spaces, water bodies, and agricultural land, representing one of the highest-density urban regions in Vietnam. According to urban development trends and planning strategies, expansion is primarily directed toward the eastern and northern areas, while the southern and northern zones retain more agricultural and ecological landscapes, offering potential for climate adaptation strategies.

Ho Chi Minh City has a typical sub-equatorial monsoon tropical climate. The city maintains high and relatively stable temperatures throughout the year, with distinct wet and dry seasons. Rapid urbanization has increased impervious surfaces and building density, contributing significantly to

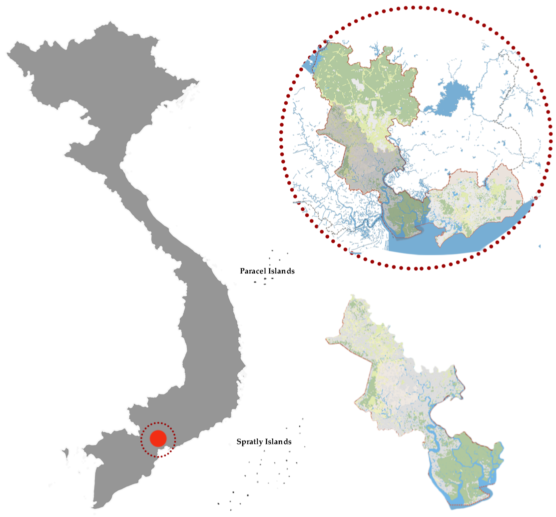

Figure 1: Location of the study area (Author, 2023, based on IGISMAP and HCMC geoportal)

Figure 2: Zoning of Ho Chi Minh City based on settlement patterns, development orientation, and administrative boundaries (Author, 2024)

the Urban Heat Island (UHI) effect. According to data from the Department of Natural Resources and Environment, the city receives abundant solar radiation with an average of 6.13 hours of sunshine per day. The annual average temperature is approximately 28.4°C. The mean temperature during hot seasons increased by at least 0.5°C between 1996 and 2000. Central urban areas recorded surface temperatures exceeding 30°C during the period 2007–2016 (Son, 2017). Furthermore, recent records from the Department of Natural Resources and Environment indicate that southern Vietnam, including Ho Chi Minh City, experienced unusually high temperatures in 2023 and 2024, approximately 1–2°C above historical averages. In April, peak daily temperatures in Ho Chi Minh City ranged from 39.4°C to 40°C (Vietnam Meteorological Agency, n.d.).

2.2. *Data pre-processing*

Different land uses and land covers result in varying patterns of heat absorption and dissipation. Land Surface Temperature (LST) is not only influenced by land cover but also by spatial configuration characteristics such as building density and vertical structure (W. Wang et al., 2008). To investigate the relationship between LST and urban metrics, this study selected five surface indicators, including NDVI, NDBI, NDWI, impervious surface, and albedo, as well as two three-dimensional explanatory variables, namely building volume and canopy height.

Among these variables, albedo is strongly related to urban three-dimensional morphology as it reflects radiative flux, which directly affects urban thermal characteristics. This reflection is influenced by vertical structural elements such as building height and urban geometry, as well as horizontal surfaces such as roofs and pavements (Hoornweg et al., 2011). NDVI, NDBI, and NDWI represent land cover characteristics capturing vegetation density, built-up intensity, and water distribution, respectively. Data were collected from multiple open sources, including the United States Geological Survey (USGS), Copernicus Data Space Ecosystem, and Google Earth Engine (GEE), and standardized to a 30 m spatial resolution (Table 1).

To avoid multicollinearity problems in the results, the Variance Inflation Factor (VIF) was calculated to assess multicollinearity in the regression. VIF threshold values differ across disciplines and studies. If VIF values exceed 7.5, multicollinearity exists among the independent variables, which may affect the reliability of the regression results (Dadashpoor et al., 2024). In Table 2, a correlation exists between NDVI and NDWI; however, the corresponding VIF values were less than 7.5. The data were not normally distributed. In addition, the boxplot diagram (Figure 3) shows that LST values exhibited moderate variation and a clear outlier, indicating the presence of some heat clusters. Impervious surface, NDBI, BV, and CH were highly skewed, suggesting heterogeneity in urban morphology, whereas albedo showed limited variation and may vary only locally.

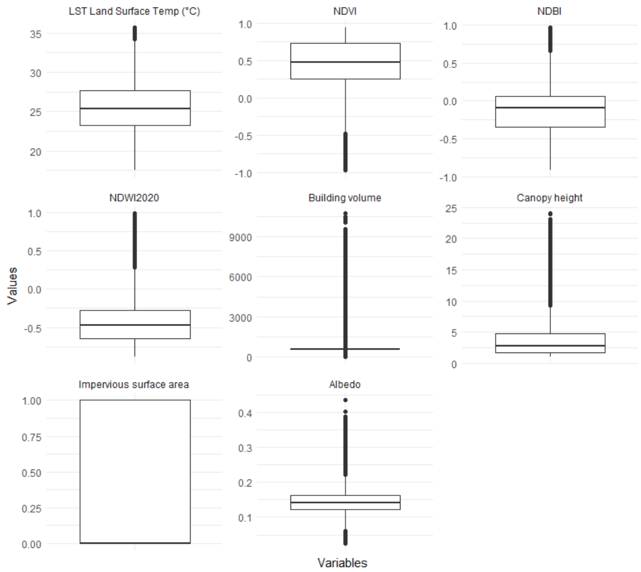

Figure 3: Boxplot of LST and independent urban variables

3. Materials and Methods

This study investigates the contributions of urban environmental indicators, including the Normalized Difference Vegetation Index (NDVI), Normalized Difference Built-up Index (NDBI), Normalized Difference Water Index (NDWI), impervious surface, building volume, canopy height, and albedo, to the spatial variability of Land Surface Temperature (LST). First, LST and urban environmental indicators were derived from remote sensing datasets using open-source geospatial databases. Subsequently, Ordinary Least Squares (OLS) regression and the Spatial Error Model (SEM) were employed and compared. Given the strong relationship between NDVI and LST, an additional SEM model incorporating a quadratic NDVI term was developed to evaluate potential improvements in model performance. Linearity, normality, homoscedasticity, spatial autocorrelation, and independence tests were conducted to validate and compare model performance. Finally, robust standard errors were applied to improve model reliability.

3.1. *Data Processing*

Landsat 8 OLI/TIRS imagery was used to derive LST in QGIS following the procedures described by (e. a. Ismaila, 2022b).

a. Spectral radiance conversion

$$L_\lambda = M_L Q_{cal} + A_L \quad (1)$$

where

- L_λ = TOA spectral radiance (W m^{-2} sr^{-1} μm^{-1})
- M_L = radiance multiplicative scaling factor
- A_L = radiance additive scaling factor
- Q_{cal} = quantized calibrated pixel value (DN)

b. Brightness temperature conversion

Table 1: Dataset used in February 2020

Data	Source	Acquired date	Res.	Metrics
LST	Landsat 8 C2 L2 (USGS)	07/02/2020	30m	2D
NDVI	Sentinel-2 (Copernicus)	25/02/2020	30m	2D
NDBI	Sentinel-2 (Copernicus)	25/02/2020	30m	2D
NDWI	Sentinel-2 (Copernicus)	25/02/2020	30m	2D
Albedo	Landsat 8 / GEE	25/02/2020	30m	2D
Building Volume	GEE derived	2020	30m	3D
Canopy Height	GEE derived	2020	30m	3D
Impervious Surface	GEE derived	25/02/2020	30m	2D

Table 2: Descriptive statistics of variables and VIF values

Variable	Min	Median	Mean	Max	VIF
LST (°C)	17.50	25.07	25.26	39.65	–
NDVI	-1.0000	0.4404	0.3751	1.0000	6.878
NDBI	-1.0000	-0.1156	-0.1345	1.0000	3.398
NDWI	-1.0000	-0.4744	-0.3656	1.0000	6.131
Building Volume	0.00	75.34	10029.01	352854.00	2.601
Canopy Height	0.000000	0.232426	1.660678	23.485882	1.462
Impervious Surface	0.0000	0.12625	0.2267	1.0000	2.724
Albedo	0.03019	0.12625	0.11808	0.20630	2.323

$$T_B = \frac{K_2}{\ln\left(\frac{K_1}{L_\lambda} + 1\right)} \tag{2}$$

where

- T_B = brightness temperature (K)
- K_1, K_2 = thermal conversion constants obtained from Landsat metadata

c. Land surface emissivity estimation

$$P_v = \left(\frac{NDVI - NDVI_{min}}{NDVI_{max} - NDVI_{min}}\right)^2 \tag{3}$$

$$\varepsilon = 0.004P_v + 0.986 \tag{4}$$

where

- P_v = vegetation proportion
- ε = land surface emissivity

d. Land Surface Temperature calculation

$$LST = \frac{T_B}{1 + \left(\frac{\lambda T_B}{\rho}\right)\ln(\varepsilon)} - 273.15 \tag{5}$$

where

- λ = wavelength of emitted radiance
- $\rho = hc/\sigma$
- h = Planck constant
- c = velocity of light
- σ = Boltzmann constant

NDVI, NDBI, and NDWI were calculated using Sentinel-2 imagery, which provides higher spatial resolution suitable for urban-scale analysis.

Normalized Difference Vegetation Index (NDVI):

$$NDVI = \frac{NIR - RED}{NIR + RED} \tag{6}$$

Normalized Difference Built-up Index (NDBI):

$$NDBI = \frac{SWIR - NIR}{SWIR + NIR} \tag{7}$$

Normalized Difference Water Index (NDWI):

$$NDWI = \frac{GREEN - NIR}{GREEN + NIR} \tag{8}$$

where

- SWIR = Band 11 (Sentinel-2)
- NIR = Band 8 (Sentinel-2)
- RED = Band 4 (Sentinel-2)
- GREEN = Band 3 (Sentinel-2)

Albedo, building volume, canopy height, and impervious surface were derived using Google Earth Engine and corresponding remote sensing products.

3.2. *Ordinary Least Squares Regression*

Ordinary Least Squares (OLS) is a widely used regression approach in spatial analysis. OLS assumes spatial independence among observations and uncorrelated residuals. The model is expressed as

$$Y = \beta_0 + \beta_1 X_1 + \beta_2 X_2 + \cdots + \beta_n X_n + \varepsilon \quad (9)$$

where Y represents LST, X_n represents the explanatory variables, β_n are regression coefficients, and ε is the random error term (Yin et al., 2018).

3.3. Spatial Error Model

Spatial regression models were employed to account for spatial dependence. The Spatial Error Model (SEM) assumes that spatial dependence exists in the error structure rather than in the dependent variable itself.

$$Y = X\beta + u \quad (10)$$

$$u = \lambda W u + \varepsilon \quad (11)$$

where Y denotes LST, X represents explanatory variables (NDVI, NDBI, NDWI, impervious surface, albedo, building volume, canopy height, and NDVI^2), λ is the spatial autoregressive coefficient, W is the spatial weight matrix; and ε is the random error term (Y. Wang et al., 2019).

3.4. Model Validation and Selection

To validate and compare the models, several diagnostic tests summarized in Table 3 were employed. A linearity test (p-value) was first applied to determine whether a linear model structure adequately captured the relationships between independent variables and Land Surface Temperature (LST). Normality was assessed using the Shapiro-Wilk Test, the Cramér-von Mises Test, and the Pearson Chi-Square Test, with corresponding test statistics and p-values. For these tests, the null hypothesis assumes that residuals are normally distributed. If $p > 0.05$, the null hypothesis is accepted, indicating normality; if $p < 0.05$, the null hypothesis is rejected, indicating non-normal residuals. Homoscedasticity was evaluated using the Breusch-Pagan Test (p-value) and the Goldfeld-Quandt Test (test statistic and p-value). If $p > 0.05$, the null hypothesis is accepted; if $p < 0.05$, heteroskedasticity is suggested. Spatial autocorrelation was assessed using Moran's I statistic. A p-value less than 0.05 indicates significant spatial dependence, suggesting that the model may not fully capture spatial effects. The independence of residuals was tested using the Durbin-Watson statistic. A value close to 2 indicates no autocorrelation, while deviations suggest residual dependence and potential violation of regression assumptions. Based on each model assumption, the appropriate tests were computed. In addition, R^2, log-likelihood, and residual Moran's I were used to evaluate model performance. A variogram was also used to compare SEM and OLS models (Siqi et al., 2023). The results indicated a strong non-linear and heteroskedastic pattern, confirming spatial heterogeneity. Finally, robust standard errors (Imbens & Kolesar, 2016) and k-fold cross-validation (A. Ismaila et al., 2023) were applied to assess the robustness and stability of the Spatial Error Model (SEM).

4. Results

4.1. Explanatory variables

Figure 4 illustrates the scatter plots of the independent variables, indicating both linear and nonlinear relationships with the dependent variable (Land Surface Temperature, LST). Several variables, including NDVI and NDWI, exhibit a negative association with LST. NDVI shows a nonlinear quadratic pattern, where LST initially increases at low vegetation coverage (NDVI ≤ 0.186) and decreases beyond this threshold. This suggests a potential nonlinear response of surface temperature to vegetation density and indicates that a simple linear specification may be insufficient. Therefore, a quadratic term is introduced and tested in the spatial regression framework. NDWI does not clearly exhibit a quadratic relationship with LST. In contrast, the built-up index (NDBI) and impervious surface show a strong and approximately linear positive relationship with LST, indicating that higher urbanization intensity is associated with increased surface temperature. Albedo shows a weak negative relationship with LST, suggesting that higher surface reflectivity contributes to surface cooling effects.

4.2. Explaining LST with the OLS model

The OLS model results (Appendix 1) indicate that all explanatory variables are statistically significant at $p < 0.01$, suggesting robust associations with LST. NDVI, NDWI, and canopy height are negatively associated with LST, while NDBI, building volume, impervious surface, and albedo exhibit positive associations. The model achieves an R^2 of 0.67, indicating that approximately 67% of the variation in LST is explained by the selected urban environmental variables. However, diagnostic tests indicate violations of key regression assumptions, particularly spatial dependence and heteroscedasticity, suggesting that OLS is insufficient for capturing the spatial structure of LST.

4.3. Explaining LST with the SEM model

In the SEM analysis, the results (see Appendix 2, 3, and 4) reveal that all explanatory variables have a statistically significant influence on land surface temperature (LST) at the 1% level ($p < 0.01$). The coefficients of NDVI and building volume are negatively associated with LST, whereas NDBI, NDWI, canopy height, impervious surface, and albedo are positively associated with LST. In the SEM, the high spatial error coefficient (λ) and the spatial autocorrelation test reported in Appendix 4 confirm the presence of spatial dependence, indicating that LST values are spatially clustered rather than randomly distributed. The model achieves an R^2 of 0.9641, a log-likelihood of −49,571.940, and an AIC of 0.9645.

In the standard SEM, NDVI exhibits a strong negative linear relationship with temperature, indicating a consistent cooling effect across space, despite the OLS results showing nonlinear curvature. To address this issue, the SEM was extended to include a quadratic NDVI specification. The coefficient of NDVI^2 provides a more detailed representation of the influence of vegetation coverage on LST, indicating

Table 3: Tests for model validation and comparison

Model	Linear Residual Test	Normality Test			Homoscedasticity Test		Spatial Correlation Test	Independence Test	AIC (Akaike Information Criterion)	R-squared
		Shapiro–Wilk Test	Cramér–von Mises Test	Pearson Chi-Square Test	Breusch–Pagan Test	Goldfeld–Quandt Test	Moran's I	Durbin–Wat–son Test		
OLS	p-value	w p-value	w p-value	w p-value	w p-value	–	–	p-value		
SEM	–	w p-value	w p-value	w p-value	w p-value	p-value	Moran's I p-value	–	–	

that the cooling efficiency of vegetation diminishes beyond a certain NDVI threshold (see Appendix 3). The SEM with quadratic NDVI shows improved model performance, with an R^2 of 0.9645, a log-likelihood of −49,203.650 (higher than −49,571.940), a lower AIC value (0.9641 compared to 0.9645), and a reduced residual variance ($\sigma^2 = 0.303$). By incorporating NDVI^2, the model better captures the nonlinear relationship between urban heat and green coverage.

4.4. Model selection

The study retained the original variables and focused on addressing the non-normality of the dataset. To assess and compare the performance of the regression models (Table 4), several diagnostic tests were conducted, including tests for linearity, normality, homoscedasticity, spatial correlation, and independence. The linearity test for the OLS model produced a low p-value ($p = 0.03566347$), indicating a significant violation of the linearity assumption. In addition, the Durbin–Watson test returned a p-value of 0, suggesting that a linear specification fails to fully capture the relationship between land surface temperature (LST) and the independent variables. Normality of residuals was assessed using the Shapiro–Wilk, Cramér–von Mises, and Pearson Chi-Square tests. Both the OLS and SEM models showed significant deviations from normality ($p < 0.05$), although the SEM slightly improved the residual distribution (Shapiro–Wilk $W = 0.95$). The SEM with quadratic NDVI further improved the result (Shapiro–Wilk $W = 0.950$); however, normality was not fully achieved.

Homoscedasticity was tested using the Breusch–Pagan and Goldfeld–Quandt tests. Across all models, the p-values were approximately zero or extremely close to zero, confirming the presence of heteroskedasticity. For spatial autocorrelation in residuals, Moran's I was employed. The OLS model exhibited clear spatial clustering in residuals, whereas both SEM specifications produced Moran's I values close to zero (approximately −0.0669 for the SEM and −0.0665 for the SEM with NDVI^2), with $p = 1$. This indicates that the SEM framework successfully accounts for spatial dependence.

Model performance was evaluated using the Akaike Information Criterion (AIC). The SEM with quadratic NDVI achieved the lowest AIC value (97232.03), outperforming the standard SEM (980073.71). Overall, the results confirm that incorporating a nonlinear NDVI term in the spatial regression model provides a more robust and reliable explanation of LST variability.

Moreover, as shown in Figure 5, the variogram comparison between OLS and SEM (with quadratic NDVI) residuals shows that the spatial regression model SEM can explain the hidden urban patterns of heat distribution with lower semi-variance across distances. This demonstrates that the SEM effectively reduces spatial autocorrelation and heteroscedasticity bias. Hence, using SEM is preferable to OLS for a more accurate explanation of urban thermal variation. Overall, with selected data, the SEM with quadratic NDVI is the most appropriate model for capturing LST variation in the HCMC case study. SEM with quadratic NDVI satisfies the model's assumptions by addressing spatial dependence and nonlinearity.

Finally, to check if the selected model can be improved further, robust standard errors were applied in the spatial regression model SEM to correct for variance inconsistency. The results in Table 5 show that both models are significant using the Wald Test and the Likelihood ratio test. Observations are correlated with values from nearby or neighboring units. However, the robust model provides a more reliable framework and achieves a slightly improved model through higher log-likelihood, a lower AIC value, and reduced residual variance.

Table 6 presents the results of the 5-fold cross-validation, where 80% of the data were used for training and 20% for testing to assess the stability and robustness of the Spatial Error Model (SEM). Across the five validation folds, the mean squared error (MSE) on the held-out samples ranged from 4.8368 to 4.9318 (°C^2). These results indicate consistent model performance across folds. The overall cross-validated error is CV(5) = 4.8836 (°C^2), corresponding to a root mean squared error (RMSE) of approximately 2.21 °C. The standard deviation of fold MSE values is low (SD = 0.0429), demonstrating that the SEM exhibits stable predictive performance. Overall, the SEM provides a stable and reliable representation of Land Surface Temperature (LST). Although the predictive accuracy is moderate, the SEM remains appropriate for spatial inference and is considered a better-fitting model under heteroskedastic conditions in the Ho Chi Minh City (HCMC) context.

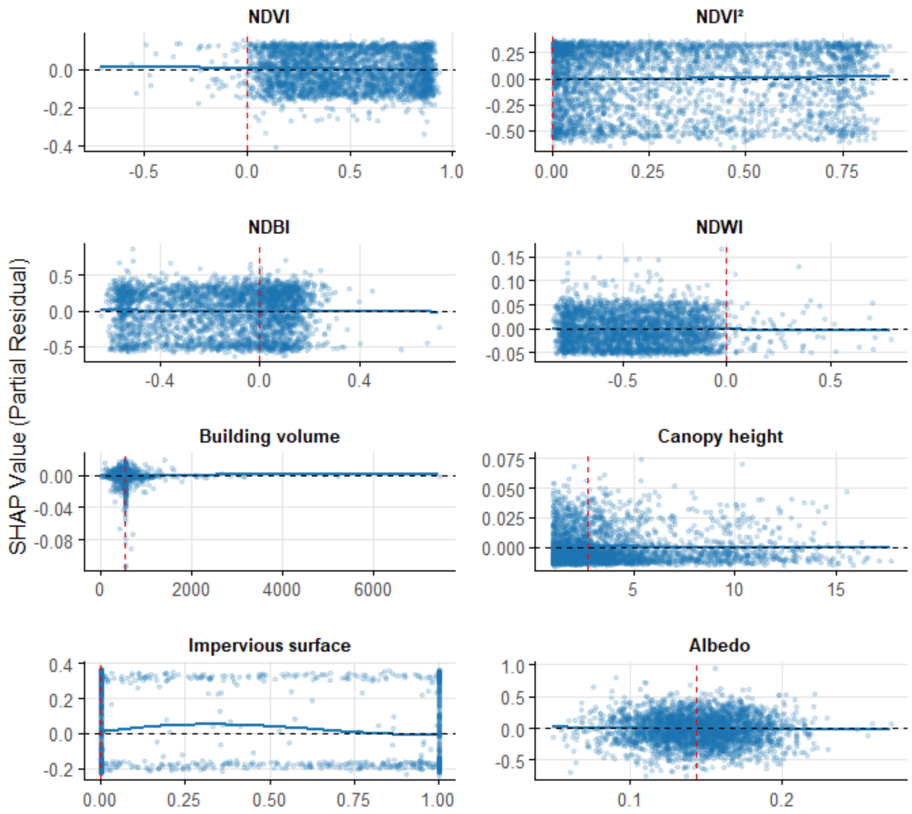

Figure 4: Relationship between LST and selected urban environmental indicators.

5. Discussion

5.1. Heat distribution in Ho Chi Minh City (HCMC)

Urbanization in Ho Chi Minh City (HCMC) has significantly altered the spatial distribution of the urban heat island (UHI). The results are consistent with previous studies on UHI patterns (T. Ha & Nguyen, 2023; A. Nguyen et al., 2023). The maximum land surface temperature (LST) is concentrated in the city center and gradually extends to surrounding areas over time, reflecting infrastructure development and the formation of industrial and residential zones. As shown in Figures 2 and Figure 6, the spatial distribution of LST in Ho Chi Minh City reveals substantial variation across urban zones. Higher LST values (above 30 °C) are concentrated in the central urban area (Zone 1) and extend toward surrounding regions, particularly the eastern region (Zone 2, Thu Duc City), which is characterized by high levels of construction activity and population density. Zone 1 and Zone 2 exhibit distinct thermal hotspots. In contrast, the northern and southern parts of the study area, especially the southern areas, show lower LST values, generally ranging between 20 °C and 25 °C, with localized hotspots reaching approximately 30 °C. These areas correspond to zones with less complex urban structures and a higher presence of cooling surfaces such as vegetation and water bodies. This spatial pattern confirms that land cover composition and urban form significantly influence surface temperature distribution, indicating that HCMC exhibits a heterogeneous and spatially dependent (heteroskedastic) thermal pattern.

5.2. Relationship of LST and urban indicators in Ho Chi Minh City

The SEM results demonstrate that selected urban environmental indicators have a significant influence on Land Surface Temperature (LST) in Ho Chi Minh City (HCMC). The results presented in Table 6 illustrate how LST responds to variations in urban environmental indicators. NDVI exhibits a non-linear relationship with LST, whereas building volume shows a statistically significant negative correlation. In contrast, canopy height, NDWI, NDBI, albedo, and impervious surface all display positive associations with LST.

NDVI has a statistically significant coefficient and a positive association with LST, indicating that at low levels of vegetation coverage, LST tends to increase slightly as NDVI increases. This suggests that sparse vegetation does not provide sufficient cooling capacity. However, the quadratic NDVI term is strongly negative, confirming a pronounced non-linear cooling effect. Once vegetation density exceeds a threshold (approximately 0.15), LST begins to decrease. This implies that effective thermal mitigation requires a minimum level of vegetation density rather than isolated or fragmented green coverage. Building volume shows a small but statistically significant negative coefficient, indicating a slight cooling effect. This may be explained by urban form configurations

Table 4: Model validation and comparison results

Model	Linear Residual Test	Normality Test			Homoscedasticity Test		Spatial Correlation Test	Independence Test	AIC	R-squared
		Shapiro–Wilk Test	Cramér–von Mises Test	Pearson Chi-Square Test	Breusch–Pagan Test	Goldfeld–Quandt Test	Moran's I	Durbin–Watson Test		
OLS	$p = 7.13 \times 10^{-163}$	$W = 0.9960$ $p < 0.001$	$W^2 = 2.961$ $p < 0.001$	$\chi^2 = 575.03$ $p < 0.001$	$p < 0.001$	–	$I = 0.33$ $p < 0.001$	$p < 0.001$	–	0.67
SEM	–	$W = 0.9404$ $p < 0.001$	$W^2 = 86.018$ $p < 0.001$	$\chi^2 = 5114$ $p < 0.001$	$p < 0.001$	$p < 0.001$	$I = -0.03$ $p < 0.001$	–	114 021	0.71
SEM + NDVI^2	–	$W = 0.9596$ $p < 0.001$	$W^2 = 80.33$ $p < 0.001$	$\chi^2 = 4994.56$ $p < 0.001$	$p < 0.001$	$p < 0.001$	$I = -0.05$ $p < 0.001$	–	110 016	0.74

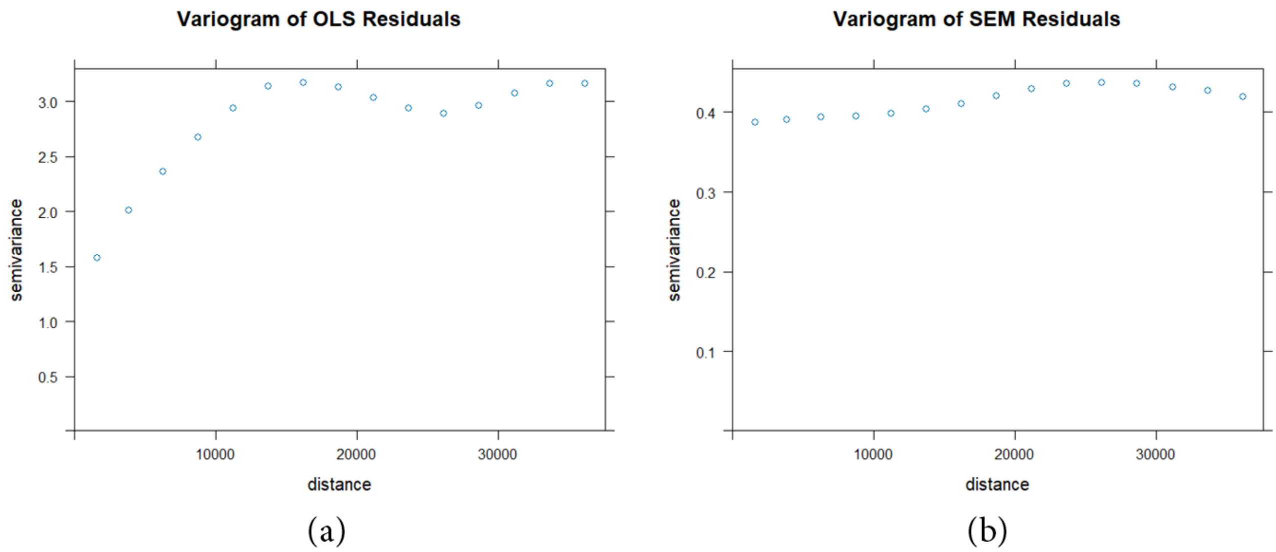

Figure 5: Variogram comparision of OLS residuals and SEM (with quaratic NDVI) residuals.

in which large building masses contribute to shading and influence air circulation patterns, thereby reducing surface temperature under certain spatial conditions.

NDBI shows a strong positive association with LST. A one-unit increase in NDBI, representing expansion of built-up areas, is associated with an increase of approximately 1.233°C in surface temperature. Similarly, impervious surface also exhibits a positive effect on LST. Impervious materials such as roads and rooftops reduce evaporation and enhance heat retention, and a one-unit increase in imperviousness leads to an approximate 0.5°C increase in temperature. Albedo also presents a strong positive coefficient with LST, indicating that high-albedo zones in the study area are dominated by heat-retaining materials. Although albedo is typically associated with cooling potential, the observed positive relationship reflects the dominance of concrete, asphalt, and construction materials in highly urbanized areas. This suggests that albedo alone is insufficient for cooling effects and must be combined with vegetation or water-based systems to achieve meaningful thermal mitigation.

Although NDWI is generally expected to be negatively correlated with LST, the results in this study show a slight positive relationship. This unexpected pattern may be explained by the complexity of dense urban environments, where mixed land cover types lead to overlapping surface thermal characteristics (Guha & Govil, 2021; Roy et al., 2022). In addition, while canopy height is often associated with cooling effects through shading, the results indicate a positive relationship with LST. This may be attributed to specific urban configurations in which dense or tall vegetation can trap longwave radiation and contribute to increased daytime surface heating. Therefore, localized and context-specific urban cooling strategies are required to effectively address thermal variation in Ho Chi Minh City.

5.3. Enhancing green and blue indicators through urban design to mitigate UHI

Under specific urban conditions, several factors contribute to the formation of Urban Heat Island (UHI), which can be categorized into controllable and uncontrollable factors. Controllable factors relate to urban planning and design, as well as pollution sources, while uncontrollable factors are caused by seasonal and transient local climate conditions, such as wind speed, wind direction, and cloud cover (Rizwan et al., 2008). Each city or neighborhood has unique climatic effects based on its individual properties and elements (Stewart & Mills, 2021a). Green and blue infrastructure plays a significant role in mitigating urban heat; however, their cooling effect depends

Table 5: Comparison of Spatial Error Model Results (ML and Robust SEs)

Variable	Coefficient	Std. Error
NDVI	0.331***	(0.039)
$I(NDVI)^2$	-1.130***	(0.047)
NDBI	1.233***	(0.033)
NDWI	0.140***	(0.020)
Building Volume	-0.00004**	(0.000014)
Canopy Height	0.004***	(0.00127)
Impervious Surface	0.508***	(0.013)
Albedo	7.758***	(0.172)
Constant	24.518***	(0.057)

Note: Values in parentheses are heteroskedasticity-consistent robust standard errors (Robust SEs) estimated using the HC1 method. Statistical significance levels: *** $p < 0.01$, ** $p < 0.05$.

Table 6: SEM validation by k-fold cross validation

Fold	Training (%)	Testing (%)	MSE (°C^2)
1	80	20	4.9318
2	80	20	4.8470
3	80	20	4.8803
4	80	20	4.8368
5	80	20	4.9223
Mean CV (5)	—	—	4.8836
SD(MSE)	—	—	0.0429
RMSE (°C)	—	—	2.2099

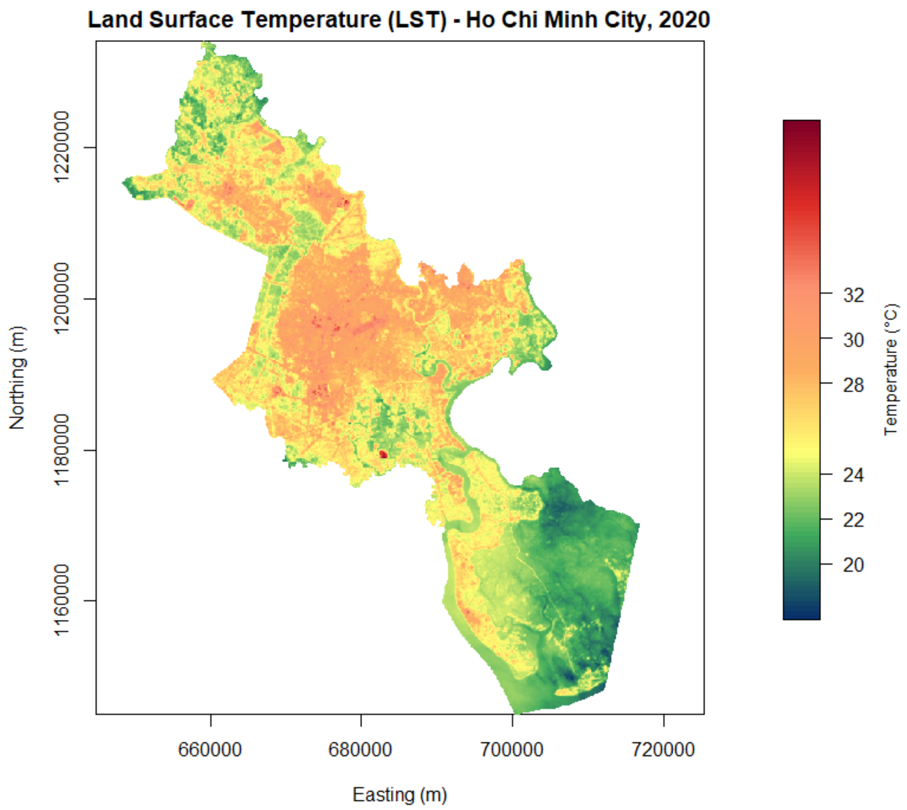

Figure 6: LST distribution of HCMC in February 2020 (Author, 2024)

on other urban environmental factors, such as building characteristics and temporal conditions (Žuvela-Aloise et al., 2016). Green factors, particularly those related to evapotranspiration and shading, which facilitate heat exchange and air movement, can effectively improve urban thermal conditions. The spatial arrangement of green spaces provides substantial cooling benefits (Yuan & Chen, 2011; Zhang, 2017).

Green blue strategies for mitigation and adaptation can be applied at multiple scales, including cities, neighborhoods, streets, and buildings, starting from the project design stage of urban planning (Table 7).

Green roofs and cool roofs are widely recognized as practical measures for mitigating urban heat and adapting to climate change. Based on solar reflection and evapotranspiration processes, both strategies have demonstrated significant effectiveness in reducing heat at the building scale, thereby modifying the microclimate (Coutts et al., 2013). Pocket parks are also considered effective solutions for improving thermal comfort in high density urban areas (Lin & Lin, 2017). In addition, enhancing urban green spaces and integrating green solutions within compact urban agglomerations are increasingly important strategies (Shih, 2017; Yuan & Chen, 2011).

The results indicate that understanding heat distribution and urban development patterns can inform planning decisions aimed at improving thermal comfort for residents. Vegetation density (NDVI), combined with vegetation structure such as canopy height, represents one of the most effective green indicators for reducing land surface temperature (LST). Canopy height can be increased through multi layered street trees and diversified tree species. Urban design can enhance NDVI by expanding vegetation coverage through green roofs, pocket parks, green walls, and connected green corridors in Ho Chi Minh City, where available land for expansion is limited. This improvement requires vegetation density to reach a threshold level (NDVI ≈ 0.15) in order to generate significant cooling effects. Cooling performance can be further improved by integrating water features such as ponds, fountains, and rain gardens, which enhance evapotranspiration when combined with vegetation. In addition, integrating green infrastructure with cooling materials, such as green roofs combined with cool pavements or solar reflective surfaces, helps reduce heat storage in the urban environment while maintaining surface cooling effects. In the context of Ho Chi Minh City, dense vegetation clusters and interconnected green networks enhance evapotranspiration processes, while shading between fragmented green spaces remains essential.

Overall, UHI mitigation in Ho Chi Minh City requires dense, well-structured, and interconnected green blue infrastructure integrated into urban design solutions within compact urban environments.

6. Conclusions

This paper describes the relationship between land surface temperature and urban environmental indicators in the high-density urban fabric of Ho Chi Minh City. The analysis reports on how to enhance urban cooling factors in the urban design process for UHI mitigation by understanding the relationship between land surface temperature and urban environment indicators. It is achieved by conducting statistical analysis, testing the traditional Ordinary Least Squares model and the Spatial Error Model based on the remote sensing process.

Results show that Ho Chi Minh City temperature increases relate to urban expansion, both with and without urban planning. UHI is concentrated in central areas and expanding to the East and North. With the complexity of urban morphology, the Spatial Error Model outperforms the Ordinary Least Squares model in capturing the relationship between land surface temperature and urban environment indicators. Vegetation index (NDVI) and building volume are two important factors that mitigate Urban Heat Island intensity through dense, structured, and connected solutions with water bodies. Optimizing green-blue infrastructure to reach the NDVI threshold and building layouts can enhance thermal comfort in dense urban areas through targeted, localized urban design solutions.

Table 7: Green and Cooling Interventions Across Urban Scales: Building, Street, Neighborhood, and City Levels

	Building	**Street**	**Neighborhood**	**City**
(1) Structure influences ventilation and airflow	Layout	Canopy layer	Layout	Layout
(2) Cover influences insulation and evaporation	Green roof, green wall, cooling devices	Street trees	Green parks, gardens	Green-blue infrastructure and the connection between water bodies and green parks
(3) Shading system / cooling system	Green roof, green wall, cooling devices, shading system	Street trees, building shading systems, cool pavements	Green parks, gardens	Green-blue infrastructure
(4) Materials and surface fabrics	High-albedo materials		Permeable paving	Lower fraction of impervious surface cover

The study sites are selected in a special urban context with high density and complex patterns. For future studies, the statistical analysis with different models can be conducted in smaller zones to optimize the quantitative relationship. Design variables must be carefully considered and calculated in detail to comprehend the complexity of urban settings and their correlations with Urban Heat Island intensity. Moreover, the measurement duration can be more diverse. These improvements help to inform design guidelines for both architects and urban planners.

Acknowledgments

The work was made possible with the support of a scholarship from the German Academic Exchange Service (DAAD).

Conflicts of Interest

The authors declare no conflict of interest.

Disclaimer/Publisher's Note

The statements, opinions, and data contained in all publications are solely those of the individual author(s) and contributor(s) and not of the Journal of Resilient Urbanism & Sustainable Design (JRUSD) and/or its editor(s). JRUSD and/or its editor(s) disclaim responsibility for any injury to individuals or damage to property resulting from any ideas, methods, instructions, or products referred to in the published content.

References

Chen, W., & Zhou, G. (2004). Spatial error model in geographic analysis. *Journal of Geographical Systems*.

Coutts, A. M., White, E. C., Tapper, N. J., Beringer, J., & Livesley, S. J. (2013). Temperature and human thermal comfort effects of street trees across three contrasting street canyon environments. *Theoretical and Applied Climatology*, *124*(1–2), 55–68. https://doi.org/10.1007/s00704-015-1409-y

Cuong & Lin. (2025). Urban heat island dynamics in ho chi minh city. *Urban Climate*.

Dadashpoor, H., et al. (2024). Assessing multicollinearity in spatial regression using vif thresholds. *Spatial Statistics*.

Downes, e. a. (2016). Urban expansion and peri-urban growth in southeast asia. *Habitat International*.

Drakakis-Smith, D., & Dixon, C. (1997). Urbanization and development in vietnam. *Urban Studies*.

Guha, S., & Govil, H. (2021). An assessment of the relationship between land surface temperature and normalized difference vegetation index. *Environment, Development and Sustainability*, *23*(2), 1944–1963.

Ha & Nguyen. (2023). Urban environmental indicators in vietnamese cities. *Journal of Environmental Management*.

Ha, T., & Nguyen, B. (2023). Spatial variation of land surface temperature in vietnam cities. *Environmental Research*, *20*(10), xx–xx.

He, e. a. (2020). Remote sensing of urban heat island using multi-indicators. *Remote Sensing*.

Hoornweg, D., et al. (2011). Cities and climate change: Global report. *World Bank Urban Development Series*.

Imbens, G. W., & Kolesar, M. (2016). Robust standard errors in small samples. *Review of Economics and Statistics*, *98*(4), 701–712. https://doi.org/10.1162/REST_a_00552

Ismaila, A., et al. (2023). K-fold cross-validation and spatial regression performance in urban environmental modeling. *Environmental Modelling & Software*.

Ismaila, e. a. (2022a). Limitations of linear regression in spatial urban analysis. *Spatial Statistics*.

Ismaila, e. a. (2022b). Spatial regression analysis in urban studies. *Spatial Statistics*.

Le, e. a. (2020). Land cover change and urban heat island effects. *Ecological Indicators*.

Lin, B. S., & Lin, Y. J. (2017). Cooling effect of shade trees with different characteristics in a subtropical urban park. *HortScience*, *45*(1), 83–86.

Mirzaei, P. A. (2015). Recent advances in modeling of urban heat island. *Urban Climate*, *10*, 38–63. https://doi.org/10.1016/j.uclim.2014.09.001

Nguyen, A., et al. (2023). Urban heat island dynamics in ho chi minh city. *Journal of Urban Climate*, *20*(10), xx–xx.

Nguyen, e. a. (2023). Remote sensing analysis of urban thermal environment. *Sustainability*.

Oliveira, V. (2016). *Urban morphology: An introduction to the study of the physical form of cities*. Springer.

Rizwan, A. M., Dennis, L. Y. C., & Liu, C. (2008). A review on the generation, determination and mitigation of urban heat island. *Journal of Environmental Sciences*, *20*(1), 120–128. https://doi.org/10.1016/S1001-0742(08)60019-4

Roy, P. S., Ramachandran, R. M., Paul, O., Thakur, P. K., Ravan, S., Behera, M. D., Sarangi, C., & Kanawade, V. P. (2022). Anthropogenic land use and land cover changes—a review on its environmental consequences and climate change. *Journal of the Indian Society of Remote Sensing*, *50*(8), 1615–1640.

Shih, W. Y. (2017). Developing green and blue infrastructure strategies for urban heat island adaptation and mitigation. *Sustainable Cities and Society*, *34*, 1–10. https://doi.org/10.1016/j.scs.2017.05.012

Son, e. a. (2017). Urbanization and spatial transformation in ho chi minh city. *Land Use Policy*.

Stewart, I. D., & Mills, G. (2021a). The urban heat island in the twenty-first century. *Urban Climate*, *37*, 100823. https://doi.org/10.1016/j.uclim.2021.100823

Stewart, I. D., & Mills, G. (2021b). Street canyon effects on urban microclimate. *Urban Forestry & Urban Greening*.

Stewart, I. D., & Mills, G. (2021c). Urban canyon geometry and thermal environment. *Building and Environment*.

Tan, H. (2020). Urban development challenges in ho chi minh city. *Vietnam Urban Review*.

Tian, e. a. (2021). Urban heat island effects on electricity consumption under climate change. *Energy Policy*.

Tuan, H., & Tran, H. (2025). Limitations of ndvi, ndwi, and ndbi in urban heat analysis. *Urban Climate Studies*.

Van Hove, L., Jacobs, J., et al. (2015). Urban heat island mitigation and climate adaptation strategies. *Urban Climate*.

Voogt, J. A., & Oke, T. R. (2003). Thermal remote sensing of urban climates. *Remote Sensing of Environment*, *86*(3), 370–384. https://doi.org/10.1016/S0034-4257(03)00079-8

Wang, W., et al. (2008). Relationships between urban form, density and land surface temperature. *Remote Sensing of Environment*.

Wang, Y., et al. (2019). Spatial regression approaches for urban heat island analysis. *Remote Sensing*.

Watkins, R., & et al. (2007). Climate change and urban health impacts. *Urban Climate and Health Studies*.

Yang & Chen. (2020). Urban form and microclimate interactions. *Landscape and Urban Planning*.

Yang, e. a. (2022). Spatial heterogeneity in environmental modeling. *Environmental Research*.

Yin, H., Kong, F., & Middel, A. (2018). Urban form and the urban heat island effect. *Sustainable Cities and Society*.

Yuan, F., & Chen, Y. (2011). Research on the cooling effects of urban parks and their relationship with urban spatial form. *Landscape and Urban Planning*, *103*(3–4), 313–321. https://doi.org/10.1016/j.landurbplan.2011.08.005

Zhang, e. a. (2017). Remote sensing indicators for urban heat island analysis. *Sustainable Cities and Society*.

Žuvela-Aloise, M., Koch, R., Buchholz, S., & Früh, B. (2016). Modelling the potential of green and blue infrastructure to reduce urban heat load in the city of vienna. *Climatic Change*, *135*(3–4), 425–438. https://doi.org/10.1007/s10584-016-1596-2

A. Appendices

Appendix 1. Ordinary Least Squares (OLS) results for LST2020

Variable	Coefficient
NDVI	-0.729*** (0.058)
NDBI	4.719*** (0.058)
NDWI	0.569*** (0.049)
BV	-0.0001*** (0.00003)
CH	-0.034*** (0.003)
Imp	2.018*** (0.022)
Albedo	13.081*** (0.287)
Constant	24.292*** (0.047)

*Note: *p<0.1; **p<0.05; ***p<0.01*

Appendix 2. Spatial Error Model (SEM) results for LST2020

Variable	Coefficient
NDVI	-0.386*** (0.021)
NDBI	1.358*** (0.025)
NDWI	0.174*** (0.017)
BV	-0.00005*** (0.00001)
CH	0.002 (0.001)
Imp	0.539*** (0.011)
Albedo	7.691*** (0.136)
Constant	24.578*** (0.055)
Observations	49,996
Log Likelihood	-49,571.940
sigma2	0.307
Akaike Info. Crit.	99,163.890
Wald Test	1,028,027.000***
LR Test	88,303.050***

*Note: *p<0.1; **p<0.05; ***p<0.01*

Appendix 3. SEM with quadratic NDVI

Variable	Coefficient
NDVI	0.331*** (0.033)
I(NDVI)^2	-1.130*** (0.041)
NDBI	1.233*** (0.025)
NDWI	0.140*** (0.017)
BV	-0.00004*** (0.00001)
CH	0.004*** (0.001)
Imp	0.508*** (0.010)
Albedo	7.758*** (0.135)
Constant	24.518*** (0.054)
Observations	49,996
Log Likelihood	-49,203.650
sigma2	0.303
Akaike Info. Crit.	98,429.310
Wald Test	1,007,693.000***
LR Test	88,072.060***

*Note: *p<0.1; **p<0.05; ***p<0.01*

Appendix 4. SEM with quadratic NDVI (HC1 robust SEs)

Variable	Coefficient
NDVI	0.331*** (0.039)
$I(NDVI)^2$	-1.130*** (0.047)
NDBI	1.233*** (0.033)
NDWI	0.140*** (0.020)
BV	-0.00004*** (0.000014)
CH	0.004** (0.00127)
Imp	0.508*** (0.013)
Albedo	7.758*** (0.172)
Constant	24.518*** (0.057)
Observations	49,996
Log Likelihood	-49,203.650
sigma2	0.303
Akaike Info. Crit.	98,429.310
Wald Test	1,007,693.000***
LR Test	88,072.060***

*Note: *p<0.1; **p<0.05; ***p<0.01*